Evaluation of ultrastructure and random effects band recovery models for estimating relationships between survival and harvest rates in exploited populations

D. L. Otis & G. C. White

Otis, D. L. & White, G. C., 2004. Evaluation of ultrastructure and random effects band recovery models for estimating relationships between survival and harvest rates in exploited populations. *Animal Biodiversity and Conservation*, 27.1: 157–173.

Abstract

Evaluation of ultrastructure and random effects band recovery models for estimating relationships between survival and harvest rates in exploited populations.— Increased population survival rate after an episode of seasonal exploitation is considered a type of compensatory population response. Lack of an increase is interpreted as evidence that exploitation results in added annual mortality in the population. Despite its importance to management of exploited species, there are limited statistical techniques for comparing relative support for these two alternative models. For exploited bird species, the most common technique is to use a fixed effect, deterministic ultrastructure model incorporated into band recovery models to estimate the relationship between harvest and survival rate. We present a new likelihood–based technique within a framework that assumes that survival and harvest are random effects that covary through time. We conducted a Monte Carlo simulation study under this framework to evaluate the performance of these two techniques. The ultrastructure models performed poorly in all simulated scenarios, due mainly to pathological distributional properties. The random effects estimators and their associated estimators of precision had relatively small negative bias under most scenarios, and profile likelihood intervals achieved nominal coverage. We suggest that the random effects estimation method approach has many advantages compared to the ultrastructure models, and that evaluation of robustness and generalization to more complex population structures are topics for additional research.

Key words: Compensatory mortality, Exploitation, Band recovery, Ultrastructure model, Random effects.

Resumen

Evaluación de los modelos ultraestructurales y de efectos aleatorios empleados en la recuperación de anillas para estimar las relaciones entre las tasas de supervivencia y las tasas de cosecha en poblaciones bajo explotación.— El aumento en la tasa de supervivencia poblacional ocurrido tras un episodio de explotación estacional se considera como un tipo de respuesta compensatoria por parte de la población. La ausencia de un aumento se interpreta como una evidencia de que la explotación se traduce en una mayor mortalidad anual de la población. Pese a su importancia para la gestión de especies bajo explotación, sólo se dispone de un número limitado de técnicas estadísticas que permiten comparar el apoyo relativo que reciben estos dos modelos alternativos. Para las especies de aves bajo explotación, la técnica más habitual consiste en utilizar un modelo de efectos fijos, de ultraestructura determinista, incorporado a los modelos de recuperación de anillas para estimar la relación entre la tasa de cosecha y la tasa de supervivencia. En el presente estudio explicamos cómo emplear una nueva técnica basada en la razón de verosimilitud, en un marco que aume que la supervivencia y la cosecha son efectos aleatorios que covarían a lo largo del tiempo. Para ello, llevamos a cabo un estudio bajo dicho marco utilizando la simulación Monte Carlo, con objeto de evaluar el rendimiento de las dos técnicas mencionadas. El rendimiento de los modelos ultraestructurales fue bastante deficiente en todos los escenarios simulados, obedeciendo, principalmente, a propiedades distribucionales patológicas. Los estimadores de efectos aleatorios y sus estimadores de precisión asociados presentaron un sesgo relativamente pequeño en la mayor parte de los escenarios, mientras que los intervalos de verosimilitud del perfil alcanzaron una cobertura nominal. Sugerimos que el planteamiento

ISSN: 1578–665X

basado en el método de estimación mediante modelos de efectos aleatorios brinda numerosas ventajas en comparación con los modelos ultraestructurales, y que la evaluación de la robustez y la generalización a estructuras poblacionales más complejas constituyen temas para una investigación adicional.

Palabras clave: Mortalidad compensatoria, Explotación, Recuperación de anillas, Modelo ultraestructural, Efectos aleatorios.

David L. Otis, U.S. Geological Survey, Biological Resources Division, Iowa Cooperative Fish and Wildlife Research Unit, 09 Science II, Iowa State Univ., Ames, IA 50011, U.S.A.– Gary C. White, Dept. of Fishery and Wildlife Biology, Colorado State Univ., Fort Collins, CO 80523 U.S.A.

Corresponding author: D. L. Otis. E–mail: dotis@iastate.edu

Introduction

Theories and models of the effects of exploitation (harvest) on vital rates of animal populations represent a fundamental and rich component of the population ecology literature. A key concept of this literature is that density dependence, effected through likely mechanisms of intraspecific competition or resource limitation, causes change in population vital rates such as survival and reproduction (Begon et al., 1996), i.e., vital rates are functions of population density. Evidence for or against hypotheses derived from this paradigm has been pursued for decades by scientists in laboratory and field studies and for all manner of taxa. Despite this effort, no general consensus or unifying principles have emerged, due to the difficulties inherent in design of critical experiments and accurate measurement of responses. Such is the case with the subject of concern in this paper, i.e., the relationship between harvest rates and vital rates of wild game bird populations.

A long history of thought and work on the degree to which bird populations compensate for seasonal harvest (Errington, 1946) continues to the present. Contemporary emphasis on this topic has focused on contrasting evidence for compensatory versus additive mortality and, to a lesser extent, density–dependent versus density–independent reproduction. In this paper, we will be concerned only with mortality rates.

A seminal paper on this topic was authored by Anderson & Burnham (1976), who developed models that related instantaneous competing mortality risks and annual rates of harvest (H) and natural (V) mortality, using a structural model that decomposed annual survival (S) into 2 seasonal components: S_h. Survival during the hunting season, and S_n. Survival during the non–hunting remainder of the year. They argued that the assumption of no natural mortality during the hunting season was mathematically reasonable, and under this simplifying assumption of temporal separation of mortality sources, $S = (1 – H) S_n$. Under the assumption of complete additivity of hunting mortality, $S_n = S_0$, where S_0 is the annual survival rate that would be realized if there were no hunting mortality (Nichols et al., 1984). Alternatively, the compensatory model is constrained by an extra parameter, usually expressed as a threshold (C).

If $H < C$, then $S_n = S_0 / (1 – H)$ and thus $S = S_0$. Nichols et al. (1984) pointed out that max $(C) = 1 – S_0$ by definition. However, the functional form of S when $H > C$ has been left unspecified in this model, other than the fact that it must be a non–increasing function of H.

Burnham et al. (1984) proposed the ultrastructure model $S = S_0 (1 – bH)$ (hereafter ultra–linear) as a general statistical model that accommodates a continuous family of relationships between harvest rate and annual survival, and allows empirical estimation of the relationship. The parameter b is interpreted as an index to the degree of dependence between S and H. When b is close to zero there is evidence for compensation and when b is close to 1, there is evidence for additivity. Note that the threshold parameter C is not incorporated into the model. Using numerical techniques, Burnham et al. (1984) produced MLE estimates $\hat{b}$ for several sets of band recovery data for adult mallards (*Anas platyrhynchos*). An associated small Monte Carlo simulation study of the statistical properties of the method suggested that $\hat{b}$ could have significant bias, the sampling distribution of $\hat{b}$ was often bimodal, and that $\widehat{se}(\hat{b})$ often exhibited significant negative bias. Several authors have subsequently employed this approach using band recovery data from waterfowl species (Barker et al., 1991; Smith & Reynolds, 1992). An alternative ultrastructure model $S = S_0 (1 – H)^b$ (hereafter ultra–power) was proposed by K. P. Burnham (Colorado State University, pers. comm.) and used by Rexstad (1992) in an analysis of Canada goose (*Branta canadensis*) band recovery data from two age classes. The author cited poor convergence rates of numerical optimization techniques in his analysis. Better performance was achieved using only the adult age class, but the author expressed reservations about the usefulness of the ultrastructure technique. Numerical instability in ultrastructure analyses of band recovery data has also been reported for black ducks (*Anas rupribes*; Conroy et al., 2002) and mourning doves (*Zenaida macroura*; Otis, 2002).

Based on this review, our assessment is that researchers interested in asking questions about density–dependent and compensatory responses to harvest mortality in game bird species have few reliable analytical tools at their disposal, and little guidance about data requirements necessary to produce reliable results from ultrastructure models. More importantly, however, we deviate from considering the relationship between harvest and survival within a fixed effect, deterministic framework, and develop an alternative technique based on the assumption that both survival and recovery rates are random variables that may covary with time (Anderson & Burnham, 1976). Conceptualization of a population survival rate as a random effect with an associated process variance has more recently been used as the basis for alternative trend estimation techniques (Franklin et al., 2002), in population viability analysis (White, 2000), and in investigation of density dependence between survival and abundance (Barker et al., 2002). Schaub & Lebreton (2004) considered the situation in which band recovery information is available on two potentially competing sources of mortality. They modelled mortality rates as random effects, and considered estimation of correlation between these processes.

We assume that harvest rate can also be considered as a random effect that covaries to some degree with survival because of an effect of harvest on survival. Deviations from this relationship due to a myriad of other biological and environmental mechanisms are modeled as random process error. Our objectives are: (1) to use Monte Carlo simulation to assess the performance characteristics of ultrastructure model estimators, and (2) to suggest and evaluate a new technique based on a random effect parameterization of band recovery data.

Estimation methods

We assume a traditional band recovery model for the situation in which N marked birds are released in each of k years, and recovery data are provided by hunters who report bands from i marked individuals in subsequent years. The recovery data are represented as $\{R_i, i = 1,...,k\}$ where the ith vector of recoveries has elements $\{r_{ij}, j = i,...,k\}$. The multinomial likelihood is parameterised by $\{S_i, i = 1,...,k-1; f_i, i = 1,...,k\}$, where S_i represents annual survival from year i to year $i + 1$ and f_i is the recovery rate in the ith hunting season. We note that recovery rate f_i is the product of the probability that a banded bird is harvested and retrieved (harvest rate; H_i) and the probability that the band is reported (λ). This model is the adult–only, time–specific Model M_1 in Brownie et al. (1985).

Ultrastructure estimation

The estimation procedure is simply to substitute the functional form for the annual survival into the multinomial likelihood function for band recovery data and use numerical techniques to find maximum likelihood estimates. For example, in the ultra–linear model, we substitute $S_i = S_0 (1 - bH_i)$, where S_0 is annual survival in the absence of harvest (assumed constant over time), b is the slope parameter, and $H_i = f_i / \lambda$. We assume here that λ is a known constant and that there is no crippling (unretrieved) loss of banded birds. Note that this model (and the ultra–power model) is not linear in the unknown parameters, and thus closed form solutions for the estimators do not exist. PROGRAM SURVIV (White, 1983) has typically been used to accomplish the estimation, but we wrote code for PROC IML (SAS Institute, 1990) using the numerical optimisation procedures contained within IML.

Estimation using a random effect model

We assume a standard single age class, year–specific band recovery model with parameterisation following Brownie et al. (1985). If annual survival rate S_i and recovery rate f_i are assumed to be fixed parameters, then the likelihood function for estimation of $\underline{S}$ and $\underline{f}$ is

$$L\left\{\underline{S},\underline{f};\underline{N},\left\{\underline{R}_i, i=1,...,k\right\}\right\} = \prod_{i=1}^{k+1} M_i\left\{N_i, R_{ij},...,R_{i,k+1};\underline{S},\underline{f}\right\} \quad (1)$$

where M_i designates the multinomial distribution for the ith cohort of released birds, N_i = size of i, j the ith cohort release, and R_{ij} = number of hunter recoveries from the ith cohort in the jth year, and there are $k + 1$ releases.

Alternatively, we assumed both survival and recovery rates were random effects. We thus conceptualised true annual survival as a process that naturally varies around some expected value, that could be modelled as a function of specific but unknown parameters. Annual recovery rate, and thereby harvest rate, was similarly considered to be a random process that varies about its expected value. Process variance for both types of parameters may be affected by biotic and abiotic factors such as weather, habitat conditions, hunting effort, or harvest regulations.

Additionally, we allowed for the possibility that these two processes may not be independent, but functionally linked. In our situation, covariance between survival and recovery (harvest) processes can be considered as an index to the relationship between survival and harvest. A process covariance of zero is consistent with the hypothesis of completely compensatory hunting mortality. If covariance is moderately negative, additive mortality is suggested. Positive covariance is biologically implausible and was not considered. Thus, our emphasis in development of an alternative technique for assessment of the relationship between harvest and survival focused on estimation of process covariance or correlation.

Let $E\{S_i\} = \mu_S$, $Var\{S_i\} = \sigma^2_S$, $E\{f_i\} = \mu_f$, $Var\{f_i\} = \sigma^2_f$, $Cov\{S_i, f_i\} = \sigma_{Sf}$, and consider the vector of MLE estimates $\underline{\hat{\Phi}}' = \left\{\hat{S}_1, \hat{f}_1, \hat{S}_2, \hat{f}_2, ..., \hat{S}_k, \hat{f}_k\right\}$ derived from the likelihood in Eq. (1).

We have $E\{\underline{\hat{\Phi}}\} = \underline{X}\,\beta$, where

$$\underline{X} = \begin{bmatrix} 1 & 0 \\ 0 & 1 \\ \vdots & \vdots \\ 1 & 0 \\ 0 & 1 \end{bmatrix} \quad \text{and} \quad \underline{\beta} = \begin{bmatrix} \mu_S \\ \mu_f \end{bmatrix}$$

The unconditional variance–covariance matrix of $\underline{\hat{\Phi}}$ is $\Delta = \Sigma + \underline{\hat{\Psi}}$, where

$$\underline{\Sigma} = \begin{bmatrix} \underline{\Lambda} & \underline{0} & \cdots & \underline{0} \\ \underline{0} & \underline{\Lambda} & \underline{0} & \cdots \\ \cdots & \underline{0} & \cdots & \underline{0} \\ \underline{0} & \cdots & \underline{0} & \underline{\Lambda} \end{bmatrix} \qquad \underline{\Lambda} = \begin{bmatrix} \sigma_S^2 & \sigma_{Sf} \\ \sigma_{Sf} & \sigma_f^2 \end{bmatrix}$$

and $\underline{\hat{\Psi}}$ is the estimated sampling variance–covariance matrix of $\underline{\hat{\Phi}}$. Using a generalized least squares approach, the normal equation for estimation of β produces the estimator

$$\underline{\hat{\beta}} = \left(\underline{X}'\underline{\Delta}^{-1}\underline{X}\right)^{-1}\underline{X}'\underline{\Delta}^{-1}\underline{\hat{\Phi}} \qquad (2)$$

subject to minimization of

$$F = \left(\underline{\hat{\Phi}} - \underline{X}\underline{\hat{\beta}}\right)'\underline{\Delta}^{-1}\left(\underline{\hat{\Phi}} - \underline{X}\underline{\hat{\beta}}\right) \qquad (3)$$

This estimator is a function of the unknown parameters σ^2_S, σ^2_f, and σ_{Sf}, and thus a solution must be obtained by using iterative techniques on Eqs. (2) and (3) to estimate these process parameters and β.

Table 1. Parameter values used in simulation of ultrastructure and MVN random effects estimators.

Tabla 1. Valores de los parámetros empleados en la simulación de los estimadores de los modelos ultraestructural y de efectos aleatorios MVN.

Parameter	Description	Values
N	Number banded and released in each year	1,000; 3,000; 5,000
Y	Number of years of banding and recovery	11; 21; 31
μ_S	True mean annual survival rate	0.30; 0.45; 0.60
μ_f	True mean annual recovery rate	0.05; 0.10; 0.15
ρ_{Sf}	True correlation between survival and recovery rate	–0.90; –0.45; 0.00
CV	Coefficient of variation of true survival and recovery rates	0.10; 0.20; 0.30

We also considered an estimator of σ^2_S, σ^2_f, and σ_{Sf}, based on the multivariate normal (MVN) likelihood:

$$L\left(\mu_S,\mu_f,\sigma^2_S,\sigma^2_f,\sigma_{Sf}\left|\underline{\hat{S}},\underline{\hat{f}},\underline{\hat{\Psi}}\right.\right)=$$

$$=\frac{\exp\left(-\frac{1}{2}\left(\hat{\Phi}-\underline{X}\beta\right)'\underline{\Delta}^{-1}\left(\hat{\Phi}-\underline{X}\beta\right)\right)}{\sqrt{(2\pi)^k\left|\underline{\Delta}\right|}},$$

where $|\Delta|$ is the determinant of Δ.

Simulation study

We investigated the statistical performance of the ultrastructure and random effects estimators using Monte Carlo simulation methods. Initial simulations of the random effects least squares estimator produced an unacceptable proportion of numerically unstable estimates, so we report only results for the MVN random effects estimator. Three values were chosen for each of the 6 necessary design parameters, resulting in 3^6 = 729 combinations. Parameter values were 6 chosen to span the range typical for banding studies of game birds (table 1). The correlation ρ_{Sf} (and hence covariance) between the survival and recovery processes were chosen to simulate a strongly additive relationship (ρ_{Sf} = –0.90), a moderately additive relationship (ρ_{Sf} = –0.45), and a completely compensatory relationship (ρ_{Sf} = 0.00).

Simulations were done in SAS (SAS Institute, 1999), using PROC IML and the nonlinear minimization algorithms available therein. Two separate SAS codes were used to simulate the two ultrastructure estimators and the MVN random effects estimator. One complete replication of the 729 scenarios (hereafter, replication) took approximately 24 hours on a 3GHz Intel processor running Windows XP for the ultrastructure simulations, and approximately 12 hours for one complete replication of the MVN simulations. Because computer time was limited, slightly fewer replications of the ultrastructure simulations were completed (see Results).

For each replication, a band recovery data set was randomly generated as follows: (1) for each year of recovery, choose a random pair of survival and recovery rates from a bivariate normal distribution parameterized by specified values of the mean vector and covariance matrix; (2) if this pair of values does not meet the multiple criteria $(1 – S) > f$, $0 < S < 1$ and $0 < f < 1$, then reject the pair and return to step 1 above; (3) for each banded cohort and recovery year, choose a random number of birds that died during the year from a binomial distribution with parameters equal to the number of individuals in the cohort that are still alive, and probability equal to 1 minus the random survival rate for that year; (4) for each banded cohort and recovery year, generate a random number of recoveries from a binomial distribution with parameters equal to the number of deaths in the cohort for that year, and probability equal to the conditional detection rate $r = f / (1 – S)$ for that year.

Given the recovery and banding data, the likelihood function for the respective methods was generated and numerical techniques used to generate point estimates of the parameters of interest.

A boundary constraint restricted the ultrastructure estimator $\hat{b}$ to (0,1). Variance estimators for the ultrastructure estimators were calculated from the Hessian matrix. For the MVN random effects estimator, profile likelihood intervals (Burnham & Anderson, 2002) for ρ_{Sf}, μ_S, μ_f, σ_S, and σ_f were derived numerically for a representative subset of the 729 scenarios based on 1,000 simulations for each scenario. Confidence interval coverage (α = 0.05) was computed for the true parameter value from which the data were simulated and also for the realized value of the five parameters for each of the simulations.

Table 2. Simulated performance statistics of the ultrastructure power model estimator $\hat{b}$. Refer to table 1 for definition of simulation design factors. Values summarized in the table are the mean of $\hat{b}$ ($\bar{\hat{b}}$), average estimated standard error [$\widehat{se}(\hat{b})$], and average empirical standard deviation of $\hat{b}$ [$\sigma(\hat{b})$] over all replications of a fixed value of the process correlation of S and f (ρ_{Sf}).

Tabla 2. Estadísticas del rendimiento simulado del estimador del modelo de potencia ultraestructural $\hat{b}$. Para una definición de los factores del diseño de simulación, véase la tabla 1. Los valores resumidos en la tabla corresponden a la media de $\hat{b}$ ($\bar{\hat{b}}$), promedio de error estándar estimado [$\widehat{se}(\hat{b})$], y promedio de desviación estándar empírica de $\hat{b}$ [$\sigma(\hat{b})$] en todas las replicaciones de un valor fijo de la correlación del proceso de S y f (ρ_{Sf}).

		ρ_{Sf} = –0.9			ρ_{Sf} = –0.45			ρ_{Sf} = 0.00		
		$\bar{\hat{b}}$	$\widehat{se}(\hat{b})$	$\sigma(\hat{b})$	$\bar{\hat{b}}$	$\widehat{se}(\hat{b})$	$\sigma(\hat{b})$	$\bar{\hat{b}}$	$\widehat{se}(\hat{b})$	$\sigma(\hat{b})$
μ_S										
	0.30	0.985	0.780	0.061	0.850	1.522	0.328	0.371	1.577	0.461
	0.45	0.988	0.441	0.049	0.796	0.961	0.388	0.313	1.105	0.442
	0.60	0.982	0.220	0.105	0.677	0.611	0.454	0.267	0.775	0.413
μ_f										
	0.05	0.973	0.992	0.102	0.779	1.802	0.393	0.360	1.946	0.463
	0.10	0.990	0.269	0.059	0.782	0.829	0.386	0.316	0.959	0.439
	0.15	0.993	0.181	0.054	0.762	0.462	0.390	0.276	0.552	0.413
CV										
	0.1	0.966	0.884	0.134	0.728	1.397	0.423	0.325	1.522	0.442
	0.2	0.993	0.388	0.047	0.788	0.979	0.381	0.309	1.076	0.433
	0.3	0.996	0.169	0.033	0.807	0.718	0.366	0.318	0.859	0.440
N										
	1,000	0.968	0.741	0.123	0.746	1.476	0.411	0.329	1.673	0.446
	3,000	0.993	0.398	0.049	0.784	0.919	0.384	0.316	1.009	0.437
	5,000	0.994	0.303	0.043	0.792	0.699	0.375	0.307	0.775	0.432
Y										
	11	0.977	0.808	0.095	0.775	1.412	0.404	0.423	1.562	0.482
	21	0.988	0.382	0.059	0.781	0.943	0.387	0.301	1.058	0.440
	31	0.989	0.252	0.060	0.766	0.739	0.380	0.228	0.837	0.393

We acknowledge two technical points about the simulation procedure relevant to expected values of the estimates. First, the average value of any of the simulation parameters for a given replication will deviate slightly from the value in table 1 because the parameter values were chosen randomly and independently in each replication. Comparisons are based on differences between an individual estimate and the relevant value in table 1. Secondly, paired random values of S and f were chosen with the constraint that (1 – S) > f. Although the theoretically logical constraint is (1 – S) > H, the range of values chosen for S and f made it very unlikely that (1 – S) < H, unless reporting rate λ was very small. Moreover, we chose to specify values of f rather than H (= f / λ) because: (1) recovery rates are commonly reported in band recovery studies and thus a reasonable range was easily determined; (2) recovery rates directly determine the number of recoveries; (3) the correlation between S and f is the same as that for S and H (assuming λ is a constant), and therefore results are invariant to choice of λ. This constraint logically induces some bias in the estimators, but we found this bias to be trivial in our interpretation of the results.

Results

Ultrastructure models

We generated 200 replications of the ultrastructure models for each of the 3^6 = 729 parameter combinations. Estimates $\hat{b}$ of the ultra–linear slope and ultra–power exponent were nearly equal in all

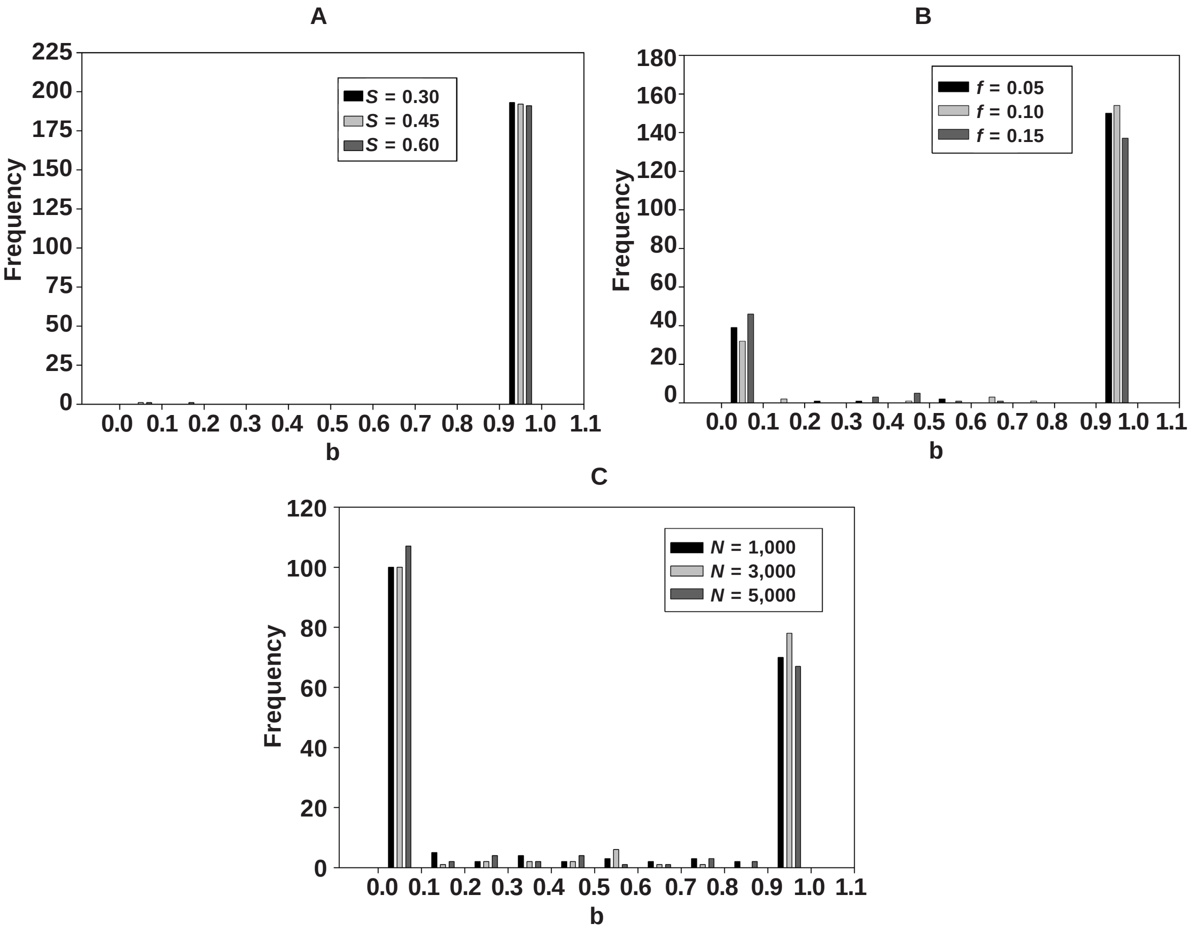

Fig. 1. Example frequency distributions of ultra–power model estimator for: A. ρ_{Sf} = –0.90, conditional on $\mu_S(S)$; B. ρ_{Sf} = –0.45, conditional on μ_f; C. ρ_{Sf} = 0.00, conditional on *N.*

Fig. 1. Ejemplo de distribuciones de frecuencia del estimador del modelo de ultra–potencia para ρ_{Sf} *= –0,90, condicionadas a* μ_{S}*(S); B.* ρ_{Sf} *= –0.45, condicionadas a* μ_{f}; C. ρ_{Sf} *= 0.00 condicionada a* N.

simulations, as were their estimated standard errors $\widehat{se}(\hat{b})$. We therefore report only results for the ultra–power model. We summarize in table 2 the mean, average estimated standard error [$\sigma(\hat{b})$], and average empirical standard deviation of $\hat{b}$ [$\widehat{se}(\hat{b})$] over all replications of a fixed value of ρ_{Sf} and a value of one other factor. Thus, each statistic is the average of 193*3^4 = 15,633 data sets.

For all cases, $\bar{\hat{b}}$ is appropriately near 1 in strongly additive cases (ρ_{Sf} = –0.9). When ρ_{Sf} = –0.45, $\bar{\hat{b}}$ was generally between 0.7 and 0.8. Because of the lack of a 1–to–1 correspondence between ρ_{Sf} and *b*, it is not possible to formally evaluate bias. However, as results are further described below, it is logical to infer that $\hat{b}$ had large positive bias in the moderately additive case. For the case of total compensation, i.e., ρ_{Sf} = 0.00, $\hat{b}$ had significant positive bias in all cases (table 2). With respect to estimates of precision, estimated sampling errors $\widehat{se}(\hat{b})$ were positively biased (relative to the empirical sampling error $\sigma(\hat{b})$ by 2–4 fold in most cases, and by an order of magnitude in several cases. For a fixed value of ρ_{Sf}, estimated sampling errors decreased as expected as simulation parameter values increase, but empirical sampling errors $\sigma(\hat{b})$ remain relatively constant, with few exceptions (table 2).

A more detailed examination of the results reveals that average values of performance metrics are very misleading because of the pathological empirical frequency istributions of the estimator in all simulated cases. Typical examples of sets of frequency distributions of $\hat{b}$ based on 193 replications each of a single combination of true parameter values are presented in fig. 1. When ρ_{Sf} = –0.9, the overwhelming majority of data sets resulted in $\hat{b}$ = 0.999 (the numerical estimation algorithm had the constraint $\hat{b}$ < 1). As previously discussed, the estimated variance of the estimator from a single replication was usually quite large, and clearly greatly overestimates the empirical variance of because of its degenerate distribution (fig. 1A). For ρ_{Sf} = –0.45, > 50%, and more typically > 80 % of $\hat{b}$ the values of $\hat{b}$ = 0.999; the remainder of the estimates were close to zero (fig. 1B). For ρ_{Sf} = 0.00, the modal value of the distribution of $\hat{b}$ was approximately zero, with a second substantial mode at 0.999.

In a multi–factor simulation study, standard statistical methods such as ANOVA or multiple regression analysis would be employed to gain insight into the parameters and combinations thereof that have the most influence on metrics such as bias and confidence interval coverage. However, we concluded that the distributional properties of $\hat{b}$ precluded both the construction of confidence intervals and attempts to conduct formal sensitivity analyses.

Informal examination of simulation results revealed that the performance of the estimator was not affected significantly by changes in values of the individual design parameters, particularly for nonzero values of ρ_{Sf}.

MVN random effects models

For each of the 3^6 = 729 scenarios shown in table 1, 250 replications were simulated. Five parameter estimates result from the estimation procedure: $\hat{\mu}_S$, $\hat{\mu}_f$, $\widehat{CV}_S$, $\widehat{CV}_f$, and $\hat{\rho}_{Sf}$. For each estimator, we summarize in table 3 the mean $[\overline{(\hat{\cdot})}]$, average estimated standard error $[\overline{\widehat{se}}(\hat{\cdot})]$, and average empirical standard deviation of $[\overline{\sigma}(\hat{\cdot})]$ conditional on a fixed value of one of the design parameters. Thus, each statistic in table 3 is generated from 250*3 = 60,750 data sets.

Table 3. Simulated performance statistics of the MVN random effects model estimators. Values summarized in the table are the mean of the estimates $[\overline{(\hat{\cdot})}]$, average estimated standard error $[\overline{\widehat{se}}(\hat{\cdot})]$, and average empirical standard deviation of $[\overline{\sigma}(\hat{\cdot})]$ conditional on a fixed value of one of the design parameters. Each entry is based on 250 replications of 3^5 = 243 scenarios, or 60,750 data sets: P. Parameter; V. Value; * Not computed.

*Tabla 3. Estadísticas del rendimiento simulado de los estimadores del modelo de efectos aleatorios MVN. Los valores resumidos en la tabla corresponden a la media de las estimaciones $[\overline{(\hat{\cdot})}]$, promedio de error estándar estimado $[\overline{\widehat{se}}(\hat{\cdot})]$, y promedio de desviación estándar empírica de $[\overline{\sigma}(\hat{\cdot})]$, condicionados a un valor fijo de uno de los parámetros del diseño. Cada entrada se basa en 250 replicaciones de 3^5 = 243 escenarios, o 60.750 conjuntos de datos: P. Parámetro; V. Valor; * No computado.*

P	V	$[\overline{(\hat{\cdot})}]$	$[\overline{\widehat{se}}(\hat{\cdot})]$	$[\overline{\sigma}(\hat{\cdot})]$
μ_S	0.30	0.297	0.0153	0.0162
	0.45	0.448	0.0213	0.0227
	0.60	0.593	0.0265	0.0285
μ_f	0.05	0.0499	0.00255	0.0027
	0.10	0.0999	0.00480	0.0051
	0.15	0.1500	0.00706	0.0075
CV_s	0.10	0.0957	*	0.0189
	0.20	0.1870	*	0.0463
	0.30	0.2783	*	0.0120
CV_f	0.10	0.0957	*	0.0084
	0.20	0.1898	*	0.0055
	0.30	0.2832	*	0.0098
ρ_{Sf}	–0.90	–0.879	0.216	0.130
	–0.45	–0.454	0.393	0.298
	0.00	–0.021	0.437	0.350

Bias

Average bias of all parameter estimates was negligible over all replications and factor combinations (table 3). We were particularly interested in estimators of ρ_{Sf}, σ_S, and σ_f, and the relative influence of the design parameters on their bias. Therefore we performed simple multi–factor ANOVAs with both bias (the average difference between the estimate and the true parameter value) and relative bias (bias / true parameter value) as the response variables, and each of the 6 design factors in the simulation study as main effects. The three factors with generally the greatest influence were number of years banded, number banded each year, and the *CV* of the survival and recovery rates. Bias of each of the estimators was generally small, but nearly always negative (table 4). The magnitude of the bias of $\hat{\rho}_{Sf}$ was not substantially influenced by the three simulation design factors. Bias of both $\hat{\sigma}_S$ and $\hat{\sigma}_f$ decreased markedly between *N* = 1,000 and *N* = 3,000, and between *Y* = 11 and *Y* = 21 (table 4).

Precision

We considered the true standard error of an estimator for a specific scenario to be the empirical standard deviation of the 250 estimates generated from the independent data sets.

Thus, for each estimator, we have 3^6 = 729 true standard errors, one for each scenario. Histograms of the true standard error of $\hat{\rho}_{Sf}$ $[\sigma(\hat{\rho}_{Sf})]$, conditional on each value of ρ_{Sf}, revealed that the frequency distribution of each $\sigma(\hat{\rho}_{Sf})$ was heavily right–skewed. The mean true standard error $[\overline{\sigma}(\hat{\rho}_{Sf})]$ of each distribution increased as ρ_{Sf} approached zero, i.e., $\overline{\sigma}(\hat{\rho}_{Sf})$ = 0.130 (ρ_{SF} = –0.90), = 0.300 (ρ_{Sf} = –0.45), = 0.350 (ρ_{Sf} = 0.00). We investigated the effects of simulation design parameters on precision of $\hat{\rho}_{Sf}$ by arbitrarily designating

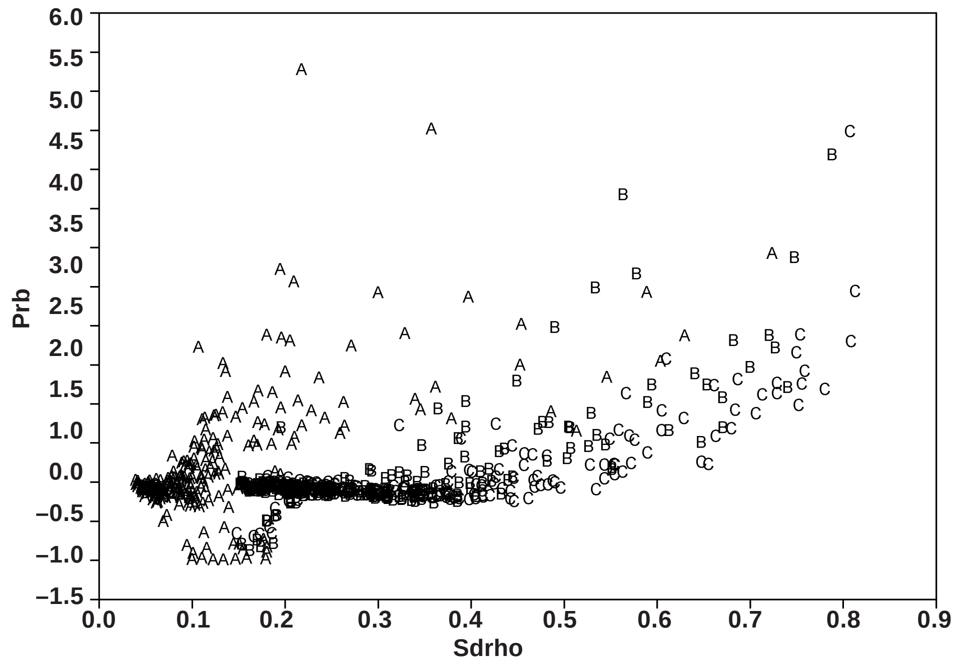

Fig. 2. Scatterplot of the percent relative bias (Prb) of the estimated average standard error of ρ_{Sf}, plotted against the empirical standard error of $\hat{\rho}_{Sf}$ (Sdrho). Each average is taken over 250 simulated data sets. Plot symbol indicates value of ρ_{Sf}: A = –0.90, B = –0.45, C = 0.00.

Fig. 2. Diagrama de dispersión del sesgo relativo porcentual (Prb) del promedio de error estándar estimado de ρ_{Sf}, representado gráficamente en comparación con el error estándar empírico de $\hat{\rho}_{Sf}$(Sdrho). Cada promedio se toma con respecto a 250 conjuntos de datos simulados. El símbolo de la representación gráfica indica el valor de ρ_{Sf}: A = –0,90; B = –0,45; C = 0,00.

$0 < \sigma(\hat{\rho}_{Sf}) < 0.20$ as an acceptable range of precision. Of the 729 simulated scenarios, there were 313 scenarios that produced acceptable precision. Increasing values of μ_S, μ_f, and *CV* were associated with slightly increased proportions of cases with acceptable precision, but design parameters ρ_{Sf} and *Y* had the largest influence: 2/3 of the acceptable scenarios had ρ_{Sf} = –0.90, and slightly more than 1/2 had *Y* = 31 (table 5).

We investigated the performance of the estimator of $\sigma(\hat{\rho}_{Sf})$, i.e., $\widehat{\mathrm{se}}(\hat{\rho}_{Sf})$, by first plotting the average relative bias $\widehat{\mathrm{se}}(\hat{\rho}_{Sf})$ of from the 250 replications of a given scenario against the corresponding $\widehat{\mathrm{se}}(\hat{\rho}_{Sf})$ (fig. 2). The estimator was generally unbiased on average when $\sigma(\hat{\rho}_{Sf}) < 0.5$, although there were several cases of large positive bias when ρ_{Sf} = –0.90. There was increasing positive bias as $\sigma(\hat{\rho}_{Sf})$ becomes large, and most of these situations occurred when ρ_{Sf} = –0.45 or ρ_{Sf} = 0.00. Generalizations are difficult to make about the combinations of the design factors that resulted in poor precision. It is generally true, however, that when at least 2 of the 3 following conditions held, estimation of precision was poor on the average: *N* = 1,000, *CV* = 0.10, *Y* = 11.

The performance of $\widehat{\mathrm{se}}(\hat{\rho}_{Sf})$ was examined in further detail by looking at the 250 individual $\widehat{\mathrm{se}}(\hat{\rho}_{Sf})$ estimates for several representative scenarios. Specifically, we were interested in the co–occurrence of poor estimates of both ρ_{Sf} and $\sigma(\hat{\rho}_{Sf})$. Unreliable results occurred when $\hat{\rho}_{Sf}$ was at a boundary value of –1.0 or 1.0. This occurred commonly under poor design scenarios (small values of *N*, *Y*, and *CV*); when ρ_{Sf} = –0.90, 66% of the estimates were at the lower boundary, and 4% were at the higher, and most of these estimates had extremely large estimated standard error. When ρ_{Sf} = 0.00, 25% of the estimates were at the lower boundary, and 18% were at the higher, with similarly large estimated standard errors. For good design scenarios, only eight of the total 500 estimates were at the negative lower bound. We suspect that these pathological individual estimates, which cause inflated average positive bias estimates, may indicate unstable performance of the numerical estimation algorithms, which we consider in more detail in the Discussion.

The estimator $\hat{\sigma}_S$ had an average percent relative bias (Prb) of ≈ –10% for above average values of σ_S (fig. 3). Prb was slightly less for smaller values of σ_S, but the estimates were more erratic. The perform-

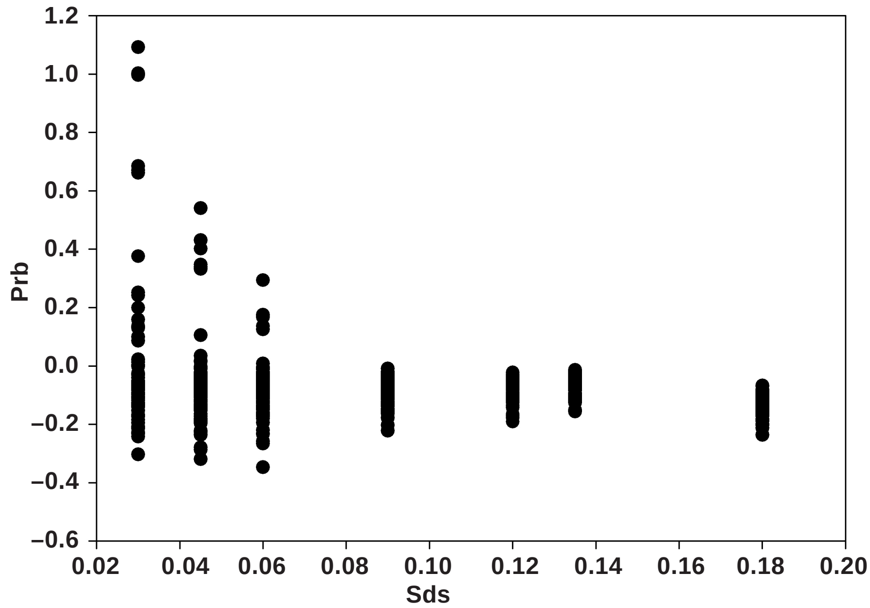

Fig. 3. Average percent relative bias (Prb) of $\hat{\sigma}_S$, plotted against σ_S (Sds). Averages are taken over 250 replications of 729 simulated scenarios.

Fig. 3. Promedio del sesgo relativo porcentual (Prb) de $\hat{\sigma}_S$, representado gráficamente en comparación con σ_S (Sds). Los promedios se toman con respecto a 250 replicaciones de 729 escenarios simulados.

ance of the estimator $\widehat{se}(\hat{\sigma}_{Sf})$, i.e., the estimated standard error of $\hat{\sigma}_S$, and the similar estimator of $\widehat{se}(\hat{\sigma}_f)$ the process recovery rate $\hat{\sigma}_f$ were better than the corresponding estimator for process correlation. Absolute percent relative bias of both estimators was generally < 10%. There were 44 scenarios for which Prb ($\widehat{se}(\hat{\sigma}_S)$) < –20%. Of these, 38 scenarios had Y = 31, CV = 0.10. Eight scenarios resulted in Prb($\widehat{se}(\hat{\sigma}_S)$) > 20%, and of these, 6 scenarios had Y = 11, CV = 0.10. There were 48 scenarios for which Prb($\widehat{se}(\hat{\sigma}_f)$) < –20%. Of these, 39 scenarios had Y = 31, CV = 0.10. Three scenarios resulted in Prb $\widehat{se}(\hat{\sigma}_f)$ > 20%, and of these, 2 scenarios had Y = 11, CV = 0.10. With respect to the general influence of the simulation design factors, Prb of both $\widehat{se}(\hat{\sigma}_S)$ and $\widehat{se}(\hat{\sigma}_f)$ was always negative when averaged over all data sets for a fixed value of a single design factor (table 6). The average Prb taken over all 729 scenarios was –7.7% for $\widehat{se}(\hat{\sigma}_S)$ and –8.0% for $\widehat{se}(\hat{\sigma}_f)$

Profile likelihood confidence interval coverage

Achieved confidence interval coverage on the value of ρ_{Sf} used to simulate the data was well below (< 75%) the nominal level of 95% for sparse data and small process variance in survival and recovery rates (table 7), i.e., N = 1000, Y = 11, and CV = 0.1. However, confidence interval coverage on ρ_{Sf} improved to ≥ 92% when $Y \geq 21$ or CV = 0.3. Confidence interval coverage on the remaining parameters was generally adequate (> 90%) with the exception of μ_f, where coverage was < 90%. Confidence interval coverage for the realized values of each simulation improved with increasing sample sizes, reaching 100% for N = 5,000 and Y = 31. It is generally true, as was also previously noted in results for precision of the estimates, that when at least 2 of the 3 following conditions hold, coverage is < 90%: N = 1,000, CV = 0.10, Y = 11.

Discussion

Limited previous evaluation of the performance of the ultrastructure estimators demonstrated negative bias in the estimators of variance (Burnham et al., 1984; Barker et al., 1991), positive bias in the estimator of the slope parameter, and a bimodal distribution for the slope estimator (Burnham et al., 1984). Unlike our study, data in these earlier studies were generated from a fixed effect ultrastructure model, so performance of the estimators was evaluated using data that conform to the true underlying model. For our study, it is straightforward to show that $E(S_i \mid f_i) = \mu_S [(1 - \rho_{Sf}) + (\rho_{Sf} / \mu_f) f_i]$. Clearly, this model structure differs from the ultrastructure models, and unless ρ_{Sf} = 0, there is no 1– to–1 correspondence between b and ρ_{Sf}. Thus, the poor performance demonstrated in our ultrastructure estimators is enhanced by differences in the true underlying data–generating model and the assumed ultrastructure model.

A second important point to consider in interpretation of ultrastructure estimator results is the constraint 0 < $\hat{b}$ < 1 used in the numerical search algorithm. This constraint significantly influenced the summary performance statistics for $\hat{b}$. For data sets in which the maximum of the likelihood occurred outside the admissible interval (and for which was therefore 0 or 1), estimated variances calculated from the Hessian matrix will be positively biased. This fact accounts for the large biases reported in table 2, and the contrast with the previous results of Burnham et al. (1984) and Barker et al. (1991), who specified larger admissible intervals for $\hat{b}$. The expected values of $\hat{b}$ for different simulation parameter sets are also differentially affected by the constraint on admissible values. For the case $b = \rho_{Sf} = 0$, we predict that the observed consistently large positive bias of $\hat{b}$ would have been even larger with an expanded interval of admissible values, because the number of estimates at the upper boundary of 1 (fig. 1C) would have been even larger. When ρ_{Sf} = –0.90, 95–99% of the estimates were at the upper bound, and the relationship between the expected value and the upper bound constraint of $\hat{b}$ is unknown in this case. It may be that the ultrastructure estimator $\hat{b}$ and its variance were well–behaved with an increased upper boundary constraint, although bias and associated interpretation of the estimates are difficult to assess under the random effects model structure. For intermediate values of ρ_{Sf}, interpretation is also difficult, but the bimodal distribution of the estimator for a given data set seems symptomatic for the ultrastructure estimator. Typically, > 10% of the estimates were at the lower bound and > 75% of the estimates were at the upper bound when ρ_{Sf} = –0.45 (fig. 1B), and we predict this "goalpost" distribution would have been exacerbated by a larger admissible boundary interval. In summary, our results demonstrate that under a random effects model, the ultrastructure model exhibited undesirable distributional properties for all scenarios except when ρ_{Sf} = –0.90, in which case results were difficult to interpret because of boundary constraints. Significant positive bias in $\hat{b}$ was documented when ρ_{Sf} = 0.00. When considered together with previous simulation evaluations and documented cases of practical application, we discourage use of the ultrastructure estimation technique in the future.

Average relative bias of the random effects estimator $\hat{\rho}_{Sf}$ was negligible for our simulated scenarios. The true variance $\sigma(\hat{\rho}_{Sf})$ of $\hat{\rho}_{Sf}$ was most significantly affected by p_{Sf}, and decreased moderately with increasing values of *N*, *CV*, and *Y*. Values of μ_S and μ_f had little effect on precision. Averaged over all values of *N, CV,* and *Y,* $\sigma(\hat{\rho}_{Sf}) \approx$ 0.35, 0.30, 0.13 for ρ_{Sf} = 0.00, –0.45, and –0.90, respectively. Thus, our random effects technique is much more sensitive in detecting a relationship between survival and harvest rates that is consistent with an additive mortality hypothesis, as opposed to the compensatory mortality hypothesis.

Table 4. Bias (B), i.e., the average difference between the estimate and the true parameter value, of estimators of process standard deviation of survival rate (σ_S), process standard deviation of recovery rate (σ_f), and process correlation between survival and recovery rate (ρ_{Sf}), conditional on values of the most influential design parameters. Each entry is based on 250 replications of 3^5 = 243 scenarios, or 60,750 data sets: F. Factor; V. Value.

Tabla 4. Sesgo (B), es decir, la diferencia media entre el valor estimado y el valor verdadero del parámetro, de los estimadores de la desviación estándar del proceso de la tasa de supervivencia (σ_S), la desviación estándar del proceso de la tasa de recuperación (σ_f), y la correlación del proceso entre la tasa de supervivencia y la tasa de recuperación (ρ_{Sf}), condicionadas a los valores de los parámetros de diseño más influyentes. Cada entrada se basa en 250 replicaciones de 3^5 = 243 escenarios, o 60.750 conjuntos de datos.

F	V	B($\hat{\sigma}_S$)	B($\hat{\sigma}_f$)	B($\sigma(\hat{\rho}_{Sf})$)
N	1,000	–0.078	–0.049	–0.016
	3,000	–0.033	–0.032	–0.006
	5,000	–0.016	–0.026	–0.002
Y	11	–0.104	–0.075	–0.031
	21	–0.048	–0.033	–0.016
	31	0.025	0.001	0.022
CV	0.1	–0.032	–0.033	–0.007
	0.2	–0.053	–0.039	–0.019
	0.3	–0.042	–0.035	–0.013

The performance of the variance estimator $\widehat{se}(\hat{\rho}_{Sf})$ was more sensitive to simulation design parameters. Minimum values of these parameters resulted in increased chance of significant bias, which was most often positive, especially when ρ_{Sf} = 0.0 or –0.45. We suspect that this result may be an artifact caused by numerical optimization problems at boundary values.

We constrained admissible values of $\hat{\rho}_{Sf}$ to the interval (–1, 1), and when estimates were at either boundary, corresponding estimates $\widehat{se}(\hat{\rho}_{Sf})$ were often very large. Investigation of improved numerical optimization techniques for the random effects procedure is a future topic of research.

As would be expected, profile likelihood confidence interval coverage improved with increasing

Table 5. Percentage (p) of n = 313 simulated cases for which the empirical standard deviation of the estimated process correlation was < 0.2, as a function of values of the simulation design parameters.

Tabla 5. Porcentaje (p) de n *= 313 casos simulados para los que la desviación estándar empírica de la correlación estimada del proceso fue < 0,2, expresada como una función de los valores de los parámetros de diseño de la simulación.*

μ_S	p	μ_f	p	CV	p	N	p	Y	p	ρ_{Sf}	p
0.30	0.31	0.05	0.28	0.10	0.26	1,000	0.22	11	0.19	–0.90	0.68
0.45	0.34	0.10	0.35	0.20	0.34	3,000	0.37	21	0.26	–0.45	0.23
0.60	0.35	0.15	0.37	0.30	0.40	5,000	0.41	31	0.55	0.00	0.09

Table 6. Average percent relative bias ($\overline{\text{Prb}}$) of the estimator $\widehat{\text{se}}(\hat{\sigma}_S)$, i.e., the standard error of the estimator of the standard deviation of the process survival rate (σ_S), and the similar estimator $\widehat{\text{se}}(\hat{\sigma}_f)$ of the process recovery rate μ_f. Each entry is based on estimates from 250 replications of 3^5 = 243 scenarios, or 60,750 data sets.

Tabla 6. Promedio de sesgo relativo porcentual ($\overline{\text{Prb}}$) del estimador $\widehat{\text{se}}(\hat{\sigma}_S)$, es decir, el error estándar del estimador de la desviación estándar de la tasa de supervivencia del proceso (σ_S), y el estimador similar $\widehat{\text{se}}(\hat{\sigma}_f)$ de la tasa de recuperación del proceso μ_f. Cada entrada se basa en estimaciones de 250 replicaciones de 3^5 = 243 escenarios, o 60.750 conjuntos de datos.

F	Value	$\overline{\text{Prb}}(\text{se}(\hat{\sigma}_S))$	$\overline{\text{Prb}}(\text{se}(\hat{\sigma}_f))$
N	1,000	–3.3	–3.8
	3,000	–9.4	–9.1
	5,000	–10.2	–11.0
Y	11	–5.4	–5.6
	21	–3.1	–3.4
	31	–14.5	–14.9
CV	0.1	–14.7	–15.3
	0.2	–5.3	–4.3
	0.3	–3.0	–4.4
ρ_{Sf}	–0.90	–9.2	–9.8
	–0.45	–6.7	–7.4
	0.00	–7.1	–6.7
μ_S	0.30	–8.3	–9.2
	0.45	–8.1	–8.2
	0.60	–6.4	–8.2
μ_f	0.05	–10.9	–11.7
	0.10	–7.4	–7.3
	0.15	–4.6	–5.0

number of years of banding. Our results suggest that Y = 11 is not adequate to obtain useful estimates of ρ_{Sf} to assess the degree of compensatory mortality operating in a populationwhen there is little process variance in survival and recovery rates. However, useful results were obtained with Y = 21, or CV = 0.3. For the limited set of scenarios simulated in table 7, the process CV is partially confounded with the number of banding occasions. However, the results presented suggest that the profile likelihood confidence interval will perform adequately for most of the 729 designs simulated in this study, with the exceptions being studies with little process variation and/or small number of banding occasions.

The random effects estimator $\hat{\sigma}_s$ had relatively small, but consistent negative bias that averaged –6.8 % over all simulations. The variance estimator of $\hat{\sigma}_s$ also performed relatively well, and had substantial negative bias only when the true relative variation in the survival process was smallest, i.e., CV = 0.10. Thus, $\hat{\sigma}_s$ can be considered an alternative to a method of moments estimator (Burnham & White, 2002) used in the technique of empirical Bayes shrinkage estimators (Burnham, unpublished manuscript), and may provide useful in applications such as minimum viable population modeling (White, 2000).

The generally satisfactory performance of the random effects method is due in large measure to the fact that the data were generated from the bivariate normal distribution, which is the underlying distribution assumed in the derivation of the estimators. Although we could have chosen alternative distributions such as logit–normal or beta with attractive attributes such as asymmetry and a (0,1) domain, we opted to use the most straightforward and easily interpretable parameter structure in this initial development and evaluation of a new method. Use of the normal distribution also allowed a clean check of whether the method was producing unbiased estimators, so that evaluation was not confounded by back–transformation complications or other factors such as the (1 – S) > f truncation constraint. The robustness of the estimators to the assumption of a bivariate normal

Table 7. Profile likelihood 95% confidence interval coverage for random effects parameters. Nominal coverage for both the true parameter value from which the recovery data were simulated and the realized value of the particular simulation are reported. Reported coverage for μ_S, μ_f, σ_S and σ_f was computed for the pooled data from the three simulated values of ρ_{Sf}: P. Parameter; TV. True value; R. Realized; NS. Number of simulations.

Tabla 7. Cobertura del perfil de intervalos de confianza al 95% para los parámetros de efectos aleatorios. Se indica la cobertura nominal para el valor verdadero del parámetro a partir del cual se simularon los datos de recuperación y el valor obtenido de la simulación concreta. Cobertura indicada para μ_S, μ_{ζ}, σ_S y σ_f se calculó para los datos combinados de los tres valores simulados de ρ_{Sf}: P. Parámetro; TV. Valor verdadero; R. Valor obtenido; NS. Número de simulaciones.

						Coverage	
N	*Y*	P	TV	CV	NS	TV	R
1,000	11	μ_S	0.30	0.1, 0.3	6,000	0.914	0.962
		μ_f	0.05	0.1, 0.3	6,000	0.849	0.931
		σ_S	0.03	0.1	3,000	0.939	0.940
				0.3	3,000	0.918	0.959
		σ_f	0.005	0.1	3,000	0.943	0.945
				0.3	3,000	0.926	0.992
		ρ_{Sf}	–0.90	0.1	1,000	0.671	0.670
				0.3	1,000	0.988	0.993
		ρ_{Sf}	–0.45	0.1	1,000	0.722	0.721
				0.3	1,000	0.927	0.967
		ρ_{Sf}	0.0	0.1	1,000	0.704	0.699
				0.3	1,000	0.934	0.977
3,000	21	μ_S	0.45	0.2	3,000	0.917	0.990
		μ_f	0.10	0.2	3,000	0.824	0.969
		σ_S	0.09	0.2	3,000	0.931	0.991
		σ_f	0.02	0.2	3,000	0.916	0.985
		ρ_{Sf}	–0.90	0.2	1,000	0.920	0.962
		ρ_{Sf}	–0.45	0.2	1,000	0.932	0.998
		ρ_{Sf}	0.0	0.2	1,000	0.949	0.999
5,000	31	μ_S	0.45	0.3	3,000	0.918	0.979
		μ_f	0.15	0.3	3,000	0.884	0.976
		σ_S	0.135	0.3	3,000	0.941	0.997
		σ_f	0.045	0.3	3,000	0.942	0.995
		ρ_{Sf}	–0.90	0.3	1,000	0.942	1.000
		ρ_{Sf}	–0.45	0.3	1,000	0.928	1.000
		ρ_{Sf}	0.0	0.3	1,000	0.933	1.000

distribution for (S, f) is of obvious importance in further development of the random effect method. However, we predict that, given a reasonable range of values for S and f, performance of the method will be more sensitive to the influential design parameters we identified than to the true underlying distribution of the random effect parameters.

There are many avenues for further investigation and development of the general random effect technique proposed here. Generalization of the models to multiple age classes should be straightforward and useful. We remain unsure about the poor performance of estimates based on a general least squares framework, but additional investiga-

Table 8. Number banded and band recoveries for female mallards banded in Wisconsin (USA) 1961–1996.

Tabla 8. Número de aves anilladas y recuperaciones de anillos correspondientes a ánades reales hembras anilladas en Wisconsin (EE.UU.) 1961–1996.

		Recoveries																
Year	Banded	61	62	63	64	65	66	67	68	69	70	71	72	73	74	75	76	77
61	2,377	76	60	53	24	10	6	8	2	4	0	0	0	0	0	0	0	0
62	2,553	0	112	91	47	15	19	11	4	0	1	0	0	0	0	0	0	0
63	1,715	0	0	107	39	13	17	16	11	6	3	0	3	1	0	0	0	0
64	986	0	0	0	54	24	29	17	6	5	0	1	1	1	0	0	0	0
65	880	0	0	0	0	33	38	13	2	2	5	1	2	1	0	0	0	0
66	2,569	0	0	0	0	0	177	71	36	19	17	7	9	5	2	0	2	0
67	1,007	0	0	0	0	0	0	55	24	14	22	9	6	7	4	0	0	0
68	1,203	0	0	0	0	0	0	0	43	29	26	14	3	6	2	0	1	0
69	867	0	0	0	0	0	0	0	0	58	33	19	6	6	0	3	1	0
70	905	0	0	0	0	0	0	0	0	0	66	21	7	7	2	0	3	1
71	747	0	0	0	0	0	0	0	0	0	0	47	18	12	2	2	5	0
72	939	0	0	0	0	0	0	0	0	0	0	0	42	25	20	15	11	3
73	666	0	0	0	0	0	0	0	0	0	0	0	0	35	18	8	2	3
74	715	0	0	0	0	0	0	0	0	0	0	0	0	0	61	17	13	7
75	627	0	0	0	0	0	0	0	0	0	0	0	0	0	0	42	18	4
76	651	0	0	0	0	0	0	0	0	0	0	0	0	0	0	0	40	11
77	1,670	0	0	0	0	0	0	0	0	0	0	0	0	0	0	0	0	107
78	1,083	0	0	0	0	0	0	0	0	0	0	0	0	0	0	0	0	0
79	646	0	0	0	0	0	0	0	0	0	0	0	0	0	0	0	0	0
80	884	0	0	0	0	0	0	0	0	0	0	0	0	0	0	0	0	0
81	1,081	0	0	0	0	0	0	0	0	0	0	0	0	0	0	0	0	0
82	947	0	0	0	0	0	0	0	0	0	0	0	0	0	0	0	0	0
83	1,193	0	0	0	0	0	0	0	0	0	0	0	0	0	0	0	0	0
84	708	0	0	0	0	0	0	0	0	0	0	0	0	0	0	0	0	0
85	584	0	0	0	0	0	0	0	0	0	0	0	0	0	0	0	0	0
86	732	0	0	0	0	0	0	0	0	0	0	0	0	0	0	0	0	0
87	786	0	0	0	0	0	0	0	0	0	0	0	0	0	0	0	0	0
88	1,923	0	0	0	0	0	0	0	0	0	0	0	0	0	0	0	0	0
89	710	0	0	0	0	0	0	0	0	0	0	0	0	0	0	0	0	0
90	1,063	0	0	0	0	0	0	0	0	0	0	0	0	0	0	0	0	0
91	1,297	0	0	0	0	0	0	0	0	0	0	0	0	0	0	0	0	0
92	1,266	0	0	0	0	0	0	0	0	0	0	0	0	0	0	0	0	0
93	1,076	0	0	0	0	0	0	0	0	0	0	0	0	0	0	0	0	0
94	820	0	0	0	0	0	0	0	0	0	0	0	0	0	0	0	0	0
95	872	0	0	0	0	0	0	0	0	0	0	0	0	0	0	0	0	0
96	529	0	0	0	0	0	0	0	0	0	0	0	0	0	0	0	0	0

Recoveries																		
78	79	80	81	82	83	84	85	86	87	88	89	90	91	92	93	94	95	96
0	0	0	0	0	0	0	0	0	0	0	0	0	0	0	0	0	0	0
0	0	0	0	0	0	1	0	0	0	0	0	0	0	0	0	0	0	0
0	0	0	0	0	0	0	0	0	0	0	0	0	0	0	0	0	0	0
0	0	0	0	0	0	0	0	0	0	0	0	0	0	0	0	0	0	0
0	0	0	0	0	0	0	0	0	0	0	0	0	0	0	0	0	0	0
0	0	0	0	0	0	0	0	0	0	0	0	0	0	0	0	0	0	0
0	0	0	0	0	0	0	0	0	0	0	0	0	0	0	0	0	0	0
0	0	0	0	0	0	0	0	0	0	0	0	0	0	0	0	0	0	0
0	0	0	0	0	0	0	0	0	0	0	0	0	0	0	0	0	0	0
0	1	0	0	0	0	0	0	0	0	0	0	0	0	0	0	0	0	0
1	0	0	0	0	0	0	0	0	0	0	0	0	0	0	0	0	0	0
2	0	0	0	0	0	0	0	0	0	0	0	0	0	0	0	0	0	0
3	0	0	0	1	0	0	0	0	0	0	0	0	0	0	0	0	0	0
5	2	1	1	0	0	0	0	0	0	0	0	0	0	0	0	0	0	0
4	3	4	2	0	0	0	0	0	0	0	0	0	0	0	0	0	0	0
10	4	3	0	0	2	0	0	0	0	0	0	0	0	0	0	0	0	0
49	30	11	4	2	8	2	1	0	0	0	1	0	0	0	0	0	0	0
84	27	11	3	6	1	1	0	0	0	0	0	0	0	0	0	0	0	0
0	53	21	7	4	2	0	1	1	0	0	1	0	0	0	0	0	0	0
0	0	50	24	9	7	4	0	1	0	1	0	0	0	0	0	0	0	0
0	0	0	61	24	10	11	2	1	3	0	0	1	0	0	0	0	0	0
0	0	0	0	68	26	11	5	5	0	0	1	0	0	0	0	0	0	0
0	0	0	0	0	121	24	11	5	5	1	1	0	2	0	0	0	0	0
0	0	0	0	0	0	61	13	4	5	0	1	0	2	0	0	0	0	0
0	0	0	0	0	0	0	21	11	4	2	2	1	0	0	0	0	0	0
0	0	0	0	0	0	0	0	39	16	6	6	1	2	2	0	0	0	0
0	0	0	0	0	0	0	0	0	32	13	6	3	2	1	0	1	2	0
0	0	0	0	0	0	0	0	0	0	59	24	18	12	7	4	3	3	1
0	0	0	0	0	0	0	0	0	0	0	18	12	9	6	5	2	2	1
0	0	0	0	0	0	0	0	0	0	0	0	52	20	5	7	3	4	0
0	0	0	0	0	0	0	0	0	0	0	0	0	67	39	18	7	5	2
0	0	0	0	0	0	0	0	0	0	0	0	0	0	60	14	9	10	7
0	0	0	0	0	0	0	0	0	0	0	0	0	0	0	43	12	8	10
0	0	0	0	0	0	0	0	0	0	0	0	0	0	0	0	42	17	11
0	0	0	0	0	0	0	0	0	0	0	0	0	0	0	0	0	32	11
0	0	0	0	0	0	0	0	0	0	0	0	0	0	0	0	0	0	39

Table 9. Results from the multivariate normal model for female mallards banded in Wisconsin (U.S.A.), 1961–1996: 95% PL. 95% profile likelihood (L. Lower; U. Upper); P. Parameter; E. Estimate; SE. Standard error.

Tabla 9. Resultados del modelo normal multivariante correspondientes a ánades reales hembras anilladas en Wisconsin (EE.UU.), 1961–1996: 95% PL. Probabilidad del perfil (L. Mínimo; U. Máximo); P. Parámetro; E. Estimación; SE. Error estándar.

			95% PL	
P	E	SE	L	U
μ_f	0.0507	0.0024	0.0496	0.0544
μ_S	0.5291	0.0147	0.4996	0.5608
σ_f	0.0126	0.0018	0.0100	0.0168
σ_S	0.0785	0.0163	0.0100	0.0679
ρ_{Sf}	–0.0197	0.2208	–0.4336	0.3934

tion may provide refinements that improve performance and result in more robust estimators. However, we suggest that a more important future study would be to investigate the performance of our technique within a density–dependent population framework. Boyce et al. (1999) characterized compensation as a demographic result of a density–dependent population mechanism, and provided a discrete–time model that incorporates seasonal harvest and density dependence that would be applicable to the situation assumed in this paper. Lebreton (unpublished manuscript) also discussed compensation as a consequence of density dependence, and argued that we should expect the quantitative relationship to be weak. He further suggested that even a weak relationship could be important to the dynamics of a population, which is consistent with our contention that the utility of our techniques or other techniques that attempt to estimate the relationship between survival and harvest should be evaluated within the context of models of the entire annual cycle of the population. Without this context, estimates of correlations or slopes cannot be practically interpreted.

Finally, we acknowledge the possible applicability of modern Bayesian or empirical Bayesian techniques to the current problem. Because of computational and philosophical issues attendant to these techniques, we chose to approach the problem from a frequentist, likelihood–based perspective. Royle & Link (2002) provide an excellent description of use of Bayesian techniques within the context of survival rate estimation from capture–recapture data.

Example

Female adult mallards were banded in Wisconsin (U.S.A.) prior to the fall hunting season during 1961–1996 (Franklin et al., 2002). Band recoveries and number banded are shown in table 8. The multivariate normal model maximum likelihood estimates and profile likelihood confidence intervals for the means and process variances are estimated with good precision (table 9). The estimate of ρ_{Sf} and its confidence interval suggest that hunting on this population during 1961–1996 was compensatory. Note that $\hat{\rho}_{Sf}$ has poor precision, which is consistent with our inference from the simulation results that precise estimation of process correlation under compensatory mortality is difficult.

Acknowledgements

We thank K. P. Burnham and J. D. Lebreton for sharing copies of unpublished manuscripts.

References

Anderson, D. R. & Burnham, K. P., 1976. Population ecology of the mallard: VI. The effect of exploitation on survival. *U.S. Fish and Wildlife Service Resource Publication,* 128.

Barker, R. J., Hines, J. E. & Nichols, J. D., 1991. Effect of hunting on annual survival of grey ducks in New Zealand. *Journal of Wildlife Management,* 55: 260–265.

Barker, R. J., Fletcher, D. & Scofield, P., 2002. Measuring density dependence in survival from capture–recapture data. *Journal of Applied Statistics,* 29: 305–313.

Begon, M., Mortimer, M. & Thompson, D. J., 1996. *Population ecology*. 3rd Ed. Blackwell Science. Oxford, U.K.

Boyce, M. S., Sinclair, A. R. E. & White, G. C. 1999. Seasonal compensation of predation and harvesting. *Oikos,* 87: 419–426.

Brownie, C. A., Anderson, D. R., Burnham, K. P., & Robson, D. S., 1985. Statistical inference from band–recovery data—a handbook. Second Edition. *U.S. Fish and Wildlife Service Resource Publication,* 131.

Burnham, K. P., White, G. C. & Anderson, D. R., 1984. Estimating the effect of hunting on annual survival rates of adult mallards. *Journal of Wildlife Management* 25, 48: 350–361.

Burnham, K. P. & Anderson, D. R., 2002. *Model selection and multimodel inference*. 2nd ed. Springer–Verlag, New York.

Burnham, K. P. & White, G. C., 2002. Evaluation of some random effects methodology applicable to bird ringing data. *Journal of Applied Statistics,* 29: 245–264.

Conroy, M. J., Miller, M. W. & Hines, J. E., 2002. Identification and synthetic modelling of factors affecting American black duck populations. *Wild-*

life Monograph, 150: 1–64.
Errington, P. L., 1946. Predation and vertebrate populations. *Quarterly Review of Biology,* 21: 144–177.
Franklin, A. B., Anderson, D. R. & Burnham, K. P., 2002. Estimation of long–term trends and variation in avian survival probabilities using random effects models. *Journal of Applied Statistics,* 29: 267–289.
Nichols, J. D., Conroy, M. J., Anderson, D. R. & Burnham, K. P., 1984. Compensatory mortality in waterfowl populations: a review of the evidence and implications for research and management. *Transactions of the North American Wildlife and Natural Resources Conference,* 49: 535–554.
Otis, D. L., 2002. Survival models for harvest management of mourning dove populations. *Journal of Wildlife Management,* 66: 1052–1063.
Rexstad, E. A., 1992. Effect of hunting on the annual survival of Canada geese in Utah. 1992. *Journal of Wildlife Management,* 56: 297–305.
Royle, J. A. & Link, W. A., 2002. Random effects and shrinkage estimation in capture–recapture models. *Journal of Applied Statistics,* 29: 329–351.
SAS Institute, 1999. *SAS/STAT Users Guid*e. Version 8. SAS Institute. Cary, North Carolina, U.S.A.
– 1990. *SAS/IML Softwar*e. Version 6. SAS Institute. Cary, North Carolina, ® U.S.A.
Schaub, M. & Lebreton, J., 2004. Testing the additive versus the compensatory hypothesis of mortality from ring recovery data using a random effects model. *Animal Biodiversity and Conservation,* 27.1: 73–85.
Smith, G. W. & Reynolds, R. E., 1992. Effect of hunting on mallard survival, 1979–1988. *Journal of Wildlife Management,* 56: 306–316.
White, G. C., 1983. Numerical estimation of survival rates from band–recovery and biotelemetry data. *Journal of Wildlife Management,* 47: 716–728.
– 2000. Population viability analysis: data requirements and essential analysis. In: *Research Techniques in Animal Ecology: Controversies and Consequence*s: 288–331 (L. Boitani & T. K. Fuller, Eds.). Columbia Univ. Press, New York.